Accepted Manuscript

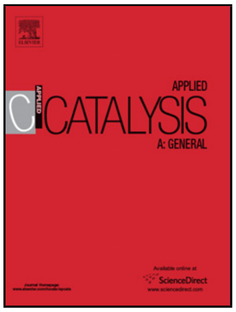

Title: Carbazole Hydrodenitrogenation over Nickel Phosphide and Ni-rich Bimetallic Phosphide Catalysts

Author: Richard H. Bowker Boris Ilic Bo.A. Carrillo Michael A. Reynolds Brendan D. Murray Mark E. Bussell

PII: S0926-860X(14)00360-3
DOI: http://dx.doi.org/doi:10.1016/j.apcata.2014.05.026
Reference: APCATA 14846

To appear in: *Applied Catalysis A: General*

Received date: 10-3-2014
Revised date: 20-5-2014
Accepted date: 23-5-2014

Please cite this article as: R.H. Bowker, B. Ilic, Bo.A. Carrillo, M.A. Reynolds, B.D. Murray, M.E. Bussell, Carbazole Hydrodenitrogenation over Nickel Phosphide and Ni-rich Bimetallic Phosphide Catalysts, *Applied Catalysis A, General* (2014), http://dx.doi.org/10.1016/j.apcata.2014.05.026

Submitted to *Applied Catalysis A*, March 10, 2014; Revised May 19, 2014.

Carbazole Hydrodenitrogenation over Nickel Phosphide and Ni-rich Bimetallic Phosphide Catalysts

Richard H. Bowker,[1,2] Boris Ilic,[1,2] Bo A. Carrillo,[1,2]
Michael A. Reynolds,[3] Brendan D. Murray[3] and Mark E. Bussell[1,2]*

[1]Department of Chemistry, MS-9150
Western Washington University
Bellingham, WA 98225

[2]Advanced Materials Science and Engineering Center
Western Washington University
Bellingham, WA 98225

[3]Shell Oil Company
Westhollow Technology Center
3333 Highway 6 South
Houston, TX 77082

*Author to whom correspondence should be addressed.

Correspondence Address

Prof. Mark E. Bussell
Department of Chemistry, MS-9150
Western Washington University
516 High Street
Bellingham, WA 98225

Tel: 360-650-3145
Fax: 360-650-2826
E-mail: Mark.Bussell@wwu.edu

Highlights

- Nickel-based phosphide catalysts out-performed a commercial Ni-Mo catalyst for carbazole HDN.

- Nickel phosphide catalysts exhibited excellent stability in a carbazole / benzothiophene feed.

- Nickel-based phosphide catalysts favored ring-opened and ring-contracted products.

- Ni_2P produced more of the partially hydrogenated hydrocarbon cyclohexylbenzene than a Ni-Mo catalyst.

ABSTRACT

Silica-supported nickel phosphide (Ni_2P) and Ni-rich bimetallic phosphide catalysts were investigated for the hydrodenitrogenation (HDN) of carbazole with and without a benzothiophene co-feed. The Ni_2P/SiO_2, $Co_{0.1}Ni_{1.9}P/SiO_2$, and $Fe_{0.03}Ni_{1.97}P/SiO_2$ catalysts exhibited high carbazole HDN activities and out-performed a commercial sulfided Ni-Mo/Al_2O_3 catalyst under the testing conditions employed. Co-feeding of benzothiophene inhibited carbazole HDN over the metal phosphides, but the Ni_2P/SiO_2 and Ni-rich bimetallic phosphide catalysts maintained higher activities than the sulfided Ni-Mo/Al_2O_3 catalyst. The product selectivities of the metal phosphide and sulfide catalysts were similar, except that the sulfided

Ni-Mo/Al_2O_3 catalyst yielded more hydrogenated carbazoles while the metal phosphide catalysts produced more of the partially hydrogenated hydrocarbon cyclohexylbenzene. The metal phosphide catalysts favored ring-opened (hexylcyclohexane) and ring-contracted ((2-methylcyclopentyl)cyclohexane) products, indicating the presence of metal and Brönsted acid sites on the catalyst surfaces. The Ni_2P/SiO_2 and bimetallic phosphide catalysts exhibited excellent stabilities in the HDN conditions employed (carbazole-only and mixed feeds), as indicated by phase purity, average crystallite size and resistance to sulfur incorporation of the supported metal phosphide particles.

KEYWORDS

Hydrodenitrogenation, HDN, carbazole, HDS, benzothiophene, nickel phosphide, bimetallic phosphide, cobalt nickel phosphide, iron nickel phosphide

1. INTRODUCTION

The removal of sulfur and nitrogen impurities from fossil fuel feedstocks is a critical processing step in producing ultralow sulfur transportation fuels [1,2]. The removal of organonitrogen compounds is necessary to achieve the ultralow sulfur levels since these compounds inhibit sulfur removal [3,4]. In addition, organonitrogen compounds poison catalysts used in down-stream refinery processes such as hydrocracking, catalytic cracking and reforming [5]. While sulfided Co-Mo/Al_2O_3 and Ni-Mo/Al_2O_3 catalysts are the workhorses of commercial hydrotreating processes, a considerable research effort is ongoing to assess the potential of alternate catalytic materials such as metal phosphides for the hydrodenitrogenation (HDN) and hydrodesulfurization (HDS) reactions [6,7]. A number of laboratories have investigated the HDS properties of the monometallic phosphides of the first-row transition metals (e.g. Ni_2P) and of MoP and WP, typically supported on silica, as well as of bimetallic phosphide materials. Among the monometallic phosphides, Ni_2P has generally been identified as being the most active for HDS of thiophene, dibenzothiophene (DBT) and 4,6-dimethyldibenzothiophene (4,6-DMDBT) [6,8-12]. Some bimetallic phosphide catalysts, Ni_2P containing a small amount of a second first-row metal (e.g. $Fe_{0.03}Ni_{1.97}P/SiO_2$ [13]), for example, have exhibited HDS activities that are higher than those of the binary phosphides of the same metals.

The HDN properties of metal phosphides have been less studied than have the HDS properties of these materials, but for feedstocks rich in nitrogen such as the Canadian oil sands [14] it is at least as important to assess the nitrogen removal capabilities of phosphide-based hydrotreating catalysts. Depending upon whether the metal phosphide was in the bulk phase or supported, and the organonitrogen compound used, MoP, Co_2P and Ni_2P have exhibited high HDN activity [8,15-17]. Consistent with what was observed for HDS, some bimetallic phosphides (Ni_xMoP, $Co_{0.4}Ni_2P$) have been observed to have HDN activities higher than those of monometallic phosphide catalysts [18,19].

While metal phosphides have exhibited promising HDS and HDN properties, evaluating their potential necessitates that they be directly compared to commercially available catalysts employed in current industrial hydrotreating applications. This study addresses this issue as metal phosphide phases supported on silica are compared to a commercial Ni-Mo/Al_2O_3 catalyst for the HDN of carbazole with and without a benzothiophene co-feed. Ni_2P and nickel-rich bimetallic phosphides (e.g. $Fe_{0.03}Ni_{1.97}P$, $Co_{0.1}Ni_{1.9}P$) show excellent promise for development into a new generation of commercial hydrotreating catalysts for hydrocarbon feeds containing high levels of nitrogen impurities.

2. EXPERIMENTAL METHODS

2.1 Catalyst Synthesis

25 wt% Ni_2P/SiO_2, $Fe_{0.03}Ni_{1.97}P/SiO_2$ and $Co_{0.1}Ni_{1.9}P/SiO_2$ catalysts were prepared from precursors having phosphorus-to-metal molar ratios (P/M) of 0.9 or 1.0 as described below. Catalyst precursors were prepared either by sequential or co-impregnation, using ammonium dihydrogen phosphate as the phosphorus salt. Following impregnation, the catalyst precursors were calcined and subjected to temperature programmed reduction (TPR) to give the metal phosphide catalysts.

Ni_2P/SiO_2. The precursor of a 25 wt% Ni_2P/SiO_2 catalyst (19.8 wt% Ni) having P/Ni = 0.9 was prepared by incipient wetness impregnation of a solution consisting of 1.9599 g nickel nitrate hexahydrate ($Ni(NO_3)_2 \cdot 6H_2O$, Alfa Aesar, 99.9985%) and 0.6978 g of ammonium dihydrogen phosphate ($NH_4H_2PO_4$, Alfa Aesar, 98%) onto 1.50 g silica support (Cab-O-Sil, M7D). Prior to impregnation, the pH of the solution was adjusted to ~2.1 to inhibit precipitate formation. The catalyst precursor was dried at 393 K for 1 h between impregnations and 24 h after the final solution addition. The dried catalyst precursor was calcined in air for 3 h at 773 K, heating from room temperature at 40 K/min. Following calcination and cooling to room temperature, approximately 0.5 g of the precursor was transferred to a quartz U-tube and degassed in 60 mL/min He (Airgas, 99.999%) for 30 min. The precursor was then subjected to TPR in H_2 (Airgas, 99.999%) flowed at 150 mL/min by heating from room temperature to 923 K at a heating rate of 1 K/min. Following TPR, the Ni_2P/SiO_2 catalyst was cooled to room temperature in continued H_2 flow, purged for 30 min in 60 mL/min He, and then passivated in 60 mL/min 1 mol% O_2/He (Airgas, 99%) for 2 h.

$Fe_{0.03}Ni_{1.97}P/SiO_2$. The precursor of a 25 wt% $Fe_{0.03}Ni_{1.97}P/SiO_2$ catalyst (0.24 wt% Fe, 19.6 wt% Ni) was prepared by impregnation of a solution containing 1.9366 g nickel nitrate and 0.0341 g iron nitrate nonahydrate ($Fe(NO_3)_3{\cdot}9H_2O$, Fischer, ACS grade) dissolved in 5 mL ultrapure water (18 MΩ resistance) onto 1.50 g of silica. The supported metal precursor was dried at 393 K between impregnations and 24 h after the final addition. A solution containing 0.7758 g ammonium dihydrogen phosphate dissolved in 4 mL ultrapure water was then impregnated onto the silica-supported iron-nickel nitrate precursor as described above to give a precursor having a P/M = 1.0. Prior to impregnation, the pH of the solutions was adjusted to ~2.1. Following drying in a 393 K oven for 24 h, the catalyst precursor was calcined, reduced via TPR, and passivated as described above.

$Co_{0.1}Ni_{1.9}P/SiO_2$. The precursor of a 25 wt% $Co_{0.1}Ni_{1.9}P/SiO_2$ catalyst (0.96 wt% Co, 18.9 wt% Ni) was prepared in a similar manner as the Ni_2P/SiO_2 catalyst, except that the impregnating solution contained 1.8628 g nickel nitrate hexahydrate, 0.0596 g cobalt nitrate hexahydrate ($Co(NO_3)_2{\cdot}6H_2O$, Alfa Aesar, ACS grade) and 0.6978 g of ammonium dihydrogen phosphate. Prior to impregnation, the pH of the solution was adjusted to ~2.1 to inhibit precipitate formation. The solution was impregnated onto 1.50 g of silica support to give a precursor having

P/M = 0.9. Following drying in a 393 K oven for 24 h, the catalyst precursor was calcined, reduced via TPR, and passivated as described above.

$Ni-Mo/Al_2O_3$. The $Ni-Mo/Al_2O_3$ catalyst used in this study was provided by Shell Oil Company (Shell 424) and had a composition of 4 wt% NiO, 19.5 wt% MoO_3 and 8 wt% P_2O_5 in its oxidic form. The $Ni-Mo/Al_2O_3$ catalyst was sulfided prior to use as described below.

2.2 Catalyst Characterization

X-ray diffraction (XRD) patterns of the as-prepared and HDN-tested Ni_2P/SiO_2, $Fe_{0.03}Ni_{1.97}P/SiO_2$ and $Co_{0.1}Ni_{1.9}P/SiO_2$ catalysts were obtained using a PANalytical X'Pert Pro diffractometer equipped with a monochromatic Cu-K_α source (λ = 1.54050 Å). BET surface area measurements were acquired using a Micromeritics PulseChemisorb 2700 instrument. Approximately 0.1000 g of catalyst was placed in a quartz sample tube and degassed at room temperature in a 60 mL/min He flow for 30 min. The sample was treated in a flow of He (45 mL/min) for 2 h at 623 K and then cooled to room temperature in a continued He flow. The BET measurements were carried out as described elsewhere [20].

Carbon monoxide (CO) and oxygen (O_2) pulsed chemisorption measurements were also obtained using the Micromeritics PulseChemisorb 2700 instrument. Approximately 0.1000 g of catalyst was degassed in 60 mL/min He at room temperature for 30 min. Prior to the measurements, the samples were either reduced (metal phosphides) or sulfided ($Ni-Mo/Al_2O_3$) in-situ. For reduction, samples were heated from room temperature to 650 K in a 60 mL/min flow of H_2 and held at this temperature for 2 h. For sulfidation, samples were heated from room temperature to 650 K in a 60 mL/min flow of a 3.0 mol% H_2S/H_2 mixture, held at this temperature for 2 h, and then reduced in a 60 mL/min flow of H_2 at 623 K for 1 h. All of the samples were then degassed in 45 mL/min He at 673 K for 1 h prior to the chemisorption measurement. CO chemisorption capacities were measured by injecting a calibrated sample volume of CO gas (Messer, 99.99%) at 1 min intervals into an He flow (45 sccm/min) passing over the catalyst sample until CO uptake ceased. Prior to injection, the CO was passed through a coil of 1/8" stainless steel tubing submerged in a pentane slush (142 K) to remove metal carbonyl impurities. Catalyst samples were maintained at a temperature of 273 K during CO chemisorption measurements. The O_2 chemisorption capacity measurements were carried out at 196 K using a procedure described elsewhere [20]. A 10.3 mol% O_2/He mixture (Airco) was used to obtain the O_2 chemisorption capacity measurements.

X-ray photoelectron spectroscopy (XPS) spectra were acquired using a SAGE 100 XPS System (SPECS GmbH) outfitted with a Mg Kα X-ray source (1253.6 eV) and a 95 mm hemispherical energy analyzer. The XPS measurements were carried out on the as-prepared Ni_2P/SiO_2, $Fe_{0.03}Ni_{1.97}P/SiO_2$, $Co_{0.1}Ni_{1.9}P/SiO_2$ catalysts following passivation and transfer through air to the spectrometer. The spectra were collected with a pass energy of 15 eV. Binding energies were corrected for sample charging using the C(1s) peak at 284.6 eV for adventitious carbon as a reference. Surface compositions were determined for the metal phosphide catalysts using SpecsLab software and the peak areas in the the Ni(3p), Co(3p), Fe(3p) and P(2p) regions.

Samples of the HDN-tested catalysts were collected for X-ray diffraction and bulk carbon and sulfur analyses. Following completion of an HDN activity measurement, the flow of liquid feed was stopped while maintaining the H_2 gas flow for 1 h at the reaction temperature. The reactor was then cooled to room temperature, depressurized, and then purged with 60 mL/min He for 30 min. The system was then opened and allowed to sit for a minimum of 3 h to permit the slow exposure of the catalyst to ambient air. Bulk carbon and sulfur analyses of HDN-tested catalyst samples were carried out using a LECO SC-144DR Sulfur and Carbon Analyzer. Approximately 0.10 g of catalyst was transferred into a ceramic boat, which was then loaded into a furnace where the sample was combusted in an oxygen-rich environment at ~1625 K for 3 min. Combusted carbon (CO_2) and sulfur (SO_2) that evolved from the catalyst sample was quantified via IR detection and reported as wt% C and S. An additional ~0.05 g sample of the HDN-tested catalysts was used to acquire an X-ray diffraction pattern as described above.

2.3 Carbazole HDN activity measurements

Carbazole HDN activity measurements were carried out using a fixed-bed, continuous flow reactor operating at a total pressure of 3.0 MPa and temperatures in the range of 548-673 K. The reactor feed consisted of either 1000 ppm carbazole and 500 ppm dodecane in a 39.85 wt% p-xylene/decane solution or 3000 ppm benzothiophene, 1000 ppm carbazole, and 500 ppm dodecane in a 39.55 wt% p-xylene/decane solution. The 500 ppm dodecane served as an internal standard for gas chromatographic analysis of the reactor effluent. The liquid feed (5.4 mL/h) was injected into a 50 mL/min flow of hydrogen and vaporized prior to entry into the reactor. 0.25 g of catalyst (16-20 mesh size) was diluted with quartz flakes to a total volume of 5 mL and loaded into a reactor tube having a diameter of 1.1 cm and length of 40 cm. The internal reactor temperature was monitored with an axially mounted thermocouple in direct contact with the catalyst bed. Metal phosphide and bimetallic phosphide catalysts were pretreated by heating from room temperature to 650 K in 1 h in a 60 mL/min flow of H_2 and held at this temperature for 2 h, then cooled to room temperature in continued H_2 flow. A commercial Ni-Mo/Al_2O_3 catalyst (Shell 424) was subjected to a sulfidation pretreatment by heating from room temperature to 650 K in 1 h in a 60 mL/min flow of 3.0 mol% H_2S/H_2 mixture, held at this temperature for 2 h, and then cooled to room temperature in continued H_2S/H_2 flow.

After pretreatment, with the catalyst samples at room temperature, the reactor was pressurized to 3.0 MPa with H_2. The catalyst bed was heated to 548 K over 15 min in a 50 mL/min flow of H_2 and liquid feed injection was begun once the reactor reached the operating temperature. The reactor was allowed to stabilize under operating conditions for 3 h prior to sampling reactor effluent at 30 min intervals over 2.5 h. The catalyst temperature was raised 25 K, the reactor stabilized for 3 h, followed by sampling of the reactor effluent at 30 min intervals. This procedure was repeated until sampling at the maximum catalyst temperature (623-673 K) was completed. The first effluent sample collected at each temperature was discarded; the four subsequent effluent samples were analyzed off-line using a gas chromatograph (Agilent 6890N) equipped with an HP-5 column and a flame ionization detector. HDN product identification was conducted by GC/MS and the GC was calibrated using serial diluted product standard solutions to allow product quantification of reactor effluent samples. Based on this method, carbon balances of 90-95% were achieved, indicating that the analyses of the reactor effluent accounted for all of the major reaction products. The majority of the HDN activity measurements were done in duplicate to ensure reproducibility.

3. RESULTS

X-ray diffraction patterns for the 25 wt% Ni_2P/SiO_2, $Fe_{0.03}Ni_{1.97}P/SiO_2$ and $Co_{0.1}Ni_{1.9}P/SiO_2$ catalysts prepared in this research are shown in Figure 1 along with a reference pattern for Ni_2P from the powder diffraction file (card no. 089-2742 [21]). For the bimetallic phosphide compositions investigated, solid solutions are formed [13,22-24], which is reflected in the XRD patterns for the $Fe_{0.03}Ni_{1.97}P/SiO_2$ and $Co_{0.1}Ni_{1.9}P/SiO_2$ catalysts closely resembling that of the Ni_2P/SiO_2 catalyst. There is no evidence in the XRD patterns for the formation of impurity phases such as the more metal-rich $Ni_{12}P_5$ (card no. 22-1190 [21]). Using the Scherrer equation and the full-width at half-maximum (FWHM) of the (111) reflection observed at ~40.8°, average crystallite sizes of 12-15 nm were calculated for the supported metal phosphide particles. Additional characterization data for the catalysts, including BET surface areas and chemisorption capacities, are listed in Table 1. The metal phosphide catalysts had similar surface areas and chemisorption (CO, O_2) capacities; the O_2 chemisorption capacities of the metal phosphide catalysts were approximately four times greater than that of the sulfided Ni-Mo/Al_2O_3 catalyst. The surface compositions of the as-prepared metal phosphide catalysts, determined using XPS, are listed in Table 1. The as-prepared Ni_2P/SiO_2, $Fe_{0.03}Ni_{1.97}P/SiO_2$ and $Co_{0.1}Ni_{1.9}P/SiO_2$ catalysts had surface compositions that were enriched in P relative to the expected stoichiometry of the bulk phase materials (P/M = 0.50); this was particularly true for the bimetallic phosphide catalysts. The amounts of Fe and Co at the surfaces of the $Fe_{0.03}Ni_{1.97}P/SiO_2$ and $Co_{0.1}Ni_{1.9}P/SiO_2$ catalysts were below the detection limit of the XPS instrument used. It should be noted that the surface compositions of the metal phosphide catalysts under reaction conditions may differ from those of the passivated catalysts measured ex situ. Previous studies in our laboratory of $Fe_xNi_{2-x}P/SiO_2$ and $Co_xNi_{2-x}P/SiO_2$ catalysts before and after HDS testing revealed the tested catalysts to have more metal-rich compositions (relative to the as-prepared catalysts) and to have low, but measureable S concentrations [13,24].

The silica-supported Ni_2P and bimetallic phosphide catalysts were tested for carbazole HDN conversion with and without a benzothiophene co-feed. The reaction network for carbazole HDN is complex and includes a number of hydrogenated carbazole compounds [3,19]). The reaction network shown in Scheme 1 is consistent with the hydrogenated carbazoles and hydrocarbon products identified via GC-MS of the liquid reactor effluent at the different reaction temperatures. In this study, the carbazole HDN conversion is defined as the conversion of carbazole and hydrogenated carbazoles to hydrocarbon products that do not contain nitrogen. For some of the catalysts investigated, the carbazole and carbazole HDN conversions differed significantly due to the presence of hydrogenated carbazoles in the reactor effluent. Shown in Figure 2 are the carbazole HDN conversions as a function of reaction temperature (498-623 K) for the Ni_2P/SiO_2, $Fe_{0.03}Ni_{1.97}P/SiO_2$ and $Co_{0.1}Ni_{1.9}P/SiO_2$ catalysts as well as for the sulfided Ni-

Mo/Al_2O_3 catalyst. All of the catalysts exhibited increasing HDN conversions with increasing temperature, with the metal phosphide catalysts having conversions ±4% of each other at each temperature. The Ni_2P/SiO_2, $Fe_{0.03}Ni_{1.97}P/SiO_2$ and $Co_{0.1}Ni_{1.9}P/SiO_2$ catalysts were more active than the sulfided Ni-Mo/Al_2O_3 catalyst in the temperature range 573-623 K. At 623 K, the metal phosphide catalysts had carbazole HDN conversions of 95% or higher while the sulfided Ni-Mo/Al_2O_3 catalyst converted 75% of the carbazole to hydrocarbon products at this same temperature. The HDN product selectivities for the catalysts will be discussed in the following section. The average crystallite sizes for the metal phosphides in the HDN-tested catalysts were unchanged, nor was there evidence for impurity phases in the XRD patterns (Figure 3 and supporting information). Carbon and sulfur analysis of the HDN-tested catalyst samples showed the metal phosphide catalysts to have carbon contents of 1-1.4 wt%. The HDN-tested sulfided Ni-Mo/Al_2O_3 catalyst had C and S contents of 1.67 and 7.10 wt%, respectively; the high sulfur content indicated that the catalyst remained sulfided despite the absence of sulfur compounds in the reactor feed.

A second set of carbazole HDN experiments, with a 3000 ppm co-feed of benzothiophene, were conducted for the Ni_2P/SiO_2, $Fe_{0.03}Ni_{1.97}P/SiO_2$, $Co_{0.1}Ni_{1.9}P/SiO_2$ and sulfided Ni-Mo/Al_2O_3 catalysts and the HDN conversion vs. temperature data for these experiments are plotted in Figure 4. Co-feeding of benzothiophene inhibited HDN of carbazole for the three metal phosphide and sulfided Ni-Mo/Al_2O_3 catalysts, particularly at low reaction temperatures. At 598 K, the Ni_2P/SiO_2, $Fe_{0.03}Ni_{1.97}P/SiO_2$ and $Co_{0.1}Ni_{1.9}P/SiO_2$ catalysts had carbazole HDN conversions of 62, 48 and 66%, respectively, with the benzothiophene co-feed, while these same catalysts had carbazole HDN conversions of 89, 96, and 89%, respectively, for the carbazole-only feed. The sulfided Ni-Mo/Al_2O_3 catalyst had carbazole HDN conversions at 598 K of 58% for the mixed feed and 73% for the carbazole-only feed. At 623 K, however, the sulfided Ni-Mo/Al_2O_3 catalyst had a higher carbazole HDN conversion of 77% vs. 75% for the carbazole-only feed, while mild inhibition of HDN activity was still observed for the metal phosphide catalysts at this temperature (Tables 2 and 3). Consistent with the carbazole HDN results for the carbazole-only feed, however, the metal phosphide catalysts were more active than the sulfided Ni-Mo/Al_2O_3 catalyst at higher temperatures (623-673 K). At 648 K, for example, the Ni_2P/SiO_2, $Fe_{0.03}Ni_{1.97}P/SiO_2$, $Co_{0.1}Ni_{1.9}P/SiO_2$ catalysts converted 97, 91 and 96% of the carbazole to hydrocarbon products, while the sulfided Ni-Mo/Al_2O_3 catalyst had a carbazole HDN conversion of 84%.

The benzothiophene HDS conversions for the mixed feed experiments over metal phosphide and sulfided Ni-Mo/Al_2O_3 catalysts are shown in Figure 5. The metal phosphide and sulfided Ni-Mo/Al_2O_3 catalysts exhibited high benzothiophene HDS conversions at temperatures of 598 K and above. A detailed analysis of the HDS product selectivity was not carried out, but the major products were identified as ethylbenzene and ethylcyclohexane.

In contrast to what was observed for the carbazole-only feed, the average crystallite sizes for the metal phosphides increased slightly from 12-15 nm in the as-prepared catalysts to 14-16 nm in the HDN-tested samples when the mixed carbazole / benzothiophene feed was used. There was no evidence for impurity phases in the XRD patterns of the HDN-tested catalysts (Figure 3, supporting information). Carbon and sulfur analysis of the HDN-tested metal phosphide catalysts revealed somewhat lower carbon contents of 0.67-1.27 wt% relative to the carbazole-only feed and low, but measurable S contents of 0.16-0.35 wt%. The sulfided Ni-Mo/Al_2O_3 catalyst also had a somewhat lower C content of 1.41 wt%, but a higher S content (8.56 wt% S) than was observed for the carbazole-only feed.

The carbazole conversions and product selectivities (mixed carbazole / benzothiophene feed) for the metal phosphide and sulfided Ni-Mo/Al_2O_3 catalysts are plotted as a function of temperature in Figures 6-9 and the selectivities for the carbzole-only and mixed feeds at 623 K are compared in Table 4. As indicated by the product selectivity data, the reaction of carbazole over the metal phosphide and sulfided Ni-Mo/Al_2O_3 catalysts yields four different hydrocarbon products – cyclohexylbenzene (CHB), bicyclohexane (BCH), (2-methylcyclopentyl)cyclohexane (MCPCH), and hexylcyclohexane (HCH) – as well as hydrogenated carbazoles (4H-CARB, 6H-CARB, 12H-CARB). Biphenyl (BP) was not observed in significant amounts (≤ 0.2 mol%). The reaction pathways leading to the different product species are summarized in the reaction network shown in Scheme 1. Focusing initially on the sulfided Ni-Mo/Al_2O_3 catalyst, hydrogenated carbazoles comprise 43 mol% of the products at 573 K but this amount decreases to 5-7 mol% at 623-673 K. The major hydrocarbon product at low temperatures (573-598 K) is bicyclohexane (30-35 mol%); however, the amount of BCH in the products decreases substantially with increasing temperature. At 623-673 K, the major product is (2-methylcyclopentyl)cyclohexane (50-55 mol%), which is formed by ring contraction of one of the six-member rings in BCH. The product selectivities for the metal phosphide catalysts exhibit qualitatively similar trends as observed for the sulfided Ni-Mo/Al_2O_3 catalyst, but with some important differences. The metal phosphides produced less hydrogenated carbazoles (< 3 mol%) at high reaction temperatures (623-673 K), resulting in higher carbazole HDN conversions, and yielded higher amounts of the partially hydrogenated product cyclohexylbenzene than did the sulfided Ni-Mo catalyst. The Ni_2P/SiO_2, $Fe_{0.03}Ni_{1.97}P/SiO_2$, $Co_{0.1}Ni_{1.9}P/SiO_2$ catalysts had CHB selectivities of 26, 30 and 32 mol% at 673 K, while the sulfided Ni-Mo/Al_2O_3 catalyst produced just 13 mol% CHB at this temperature.

The HDN product selectivities are listed in Table 4 for the carbazole-only and mixed feeds at a reaction temperature of 623 K, showing how benzothiophene affects product selectivity. Significant differences in the HDN product selectivities are apparent when comparing the two different feeds, with similar changes observed for the sulfided Ni-Mo/Al_2O_3 and metal phosphide catalysts. When benzothiophene is present in the reactor feed, the selectivity towards BCH decreased from 33-40 mol% to 22-29 mol%, while the selectivities towards CHB, MCPCH and HCH increased by approximately the same amount in total. As indicated in Scheme 1, MCPCH and HCH are products formed via ring contraction and ring opening, respectively, of one of the six-member rings of BCH.

4. DISCUSSION

The catalytic removal of nitrogen in crude oil fractions via HDN reactions is critical in the production of ultra-low sulfur fuels since organonitrogen compounds inhibit HDS and other oil conversion reactions [3,5]. For hydrotreating reactions, strong adsorption of organonitrogen molecules on catalyst surfaces blocks active sites for HDS and can limit the supply of available hydrogen species [4]. This is particularly problematic for HDS of refractory sulfur compounds such as 4,6-DMDBT. Nitrogen-containing compounds in crude oil can be divided into basic and non-basic compounds, with the basic compounds consisting primarily of molecules containing six-membered N-containing rings (e.g. quinoline) and the non-basic compounds generally consisting of molecules having five-membered N-containing rings (e.g. carbazole). Studies have shown that crude oil fractions from different sources contain different amounts and distributions of organonitrogen compounds. Heavier feeds typically contain higher levels of nitrogen (and sulfur) compounds [3]. Middle distillate cuts from shale oil and petroleum were observed to contain predominantly pyridine compounds (six-membered N rings) while the same cut from a Canadian oil sands-derived feed showed higher levels of indole and carbazole compounds (five-membered N rings) than pyridines [3,25]. Carbazole and alkyl-substituted carbazoles are among the most refractory organonitrogen compounds and, for this reason, carbazole was selected as the model compound for this HDN study.

Conventional Ni-Mo sulfide catalysts used in hydrotreating frequently contain phosphorus as an additive, most frequently for HDN processing due to the stronger promotion of HDN activity than of HDS. Indeed, the commercial Ni-Mo/Al_2O_3 catalyst used in this study contained 8 wt% P_2O_5, which corresponds to a phosphorus-to-metal mole ratio (P/(Ni+Mo)) of 0.6. The properties of phosphorus as a promoter of sulfide-based hydrotreating catalysts have been discussed in reviews by others [3,26,27]. Phosphorus is typically added to the impregnation solution in the form of phosphate (e.g. H_3PO_4, $NH_4H_2PO_4$), resulting in increased solubility of molybdate salts via formation of phosphomolybdate species. A number of explanations have been advanced to explain the promotional effect of P on HDN activity including morphological changes of the MoS_2 crystallites (increased stacking of MoS_2 layers), leading to increased hydrogenation activity, and the formation of highly dispersed Ni and/or Mo phosphides (or phosphosulfides) at the edges of the MoS_2 under reaction conditions [3,26,27].

Oxide-supported metal phosphides represent a possible step-out catalyst development technology for the removal of S and N impurities from crude oil feedstocks. The goal of the current study was to compare the catalytic properties of silica-supported nickel phosphide and Ni-rich bimetallic phosphides with those of a commercial Ni-Mo sulfide catalyst for the HDN of carbazole. The key finding of this study is that Ni_2P/SiO_2 and Ni-rich bimetallic phosphide ($Fe_{0.03}Ni_{1.97}P/SiO_2$, $Co_{0.1}Ni_{1.9}P/SiO_2$) are highly active and stable HDN catalysts, with properties superior to those of a commercial sulfided Ni-Mo/Al_2O_3 catalyst under the reaction conditions employed. Studies of carbazole HDN over unsupported and supported metal phosphides have been reported [18,19]. For a series of unsupported Ni_xMoP catalysts ($0 \leq x \leq 1.11$), Abu and Smith measured significantly higher carbazole conversions (>85%) for bimetallic Ni_xMoP

phases than for MoP (54.5%) at 583 K on a mass of catalyst basis [19]. The most active phosphide, $Ni_{0.07}MoP$, produced mostly BCH (85.6%) with smaller amounts of 4H-CARB (7.9%) and isomerized or cracked hydrocarbon products. The higher HDN activities of the Ni_xMoP catalysts relative to MoP were attributed to enhanced hydrogenation properties for the Ni-containing phosphides. For alumina-supported phases, $Co_{0.4}Ni_2P/Al_2O_3$ and $Ni_{0.3}MoP/Al_2O_3$ exhibited high HDN activity for carbazole, but the Mo-based phosphide was the more active of the two [18]. This carried over for a mixed light gas oil feed for which the $Ni_{0.3}MoP/Al_2O_3$ catalyst was more active and the $Co_{0.4}Ni_2P/Al_2O_3$ was less active than a sulfided Ni-Mo/Al_2O_3 catalyst.

In the present study, Ni_2P/SiO_2, $Fe_{0.03}Ni_{1.97}P/SiO_2$, $Co_{0.1}Ni_{1.9}P/SiO_2$ catalysts exhibited higher carbazole HDN conversions than a sulfided Ni-Mo/Al_2O_3 catalyst (for the same mass of catalyst) using both carbazole-only and mixed carbazole / benzothiophene feeds. Of particular importance, the maximum carbazole HDN conversions achieved for the metal phosphide catalysts (92-98%) were significantly higher than those of the sulfided Ni-Mo/Al_2O_3 catalyst (75-84%) for both feeds. In addition, the nickel phosphide and Ni-rich bimetallic phosphide catalysts yielded substantially higher amounts of partially-hydrogenated hydrocarbon products than did the sulfide catalyst, therefore consuming less hydrogen while achieving the higher HDN conversions. The metal phosphide catalysts also exhibited excellent stability, as indicated by no loss of phase purity and minimal increase in average crystallite size, as well as minimal S incorporation in the catalysts for the mixed carbazole / benzothiophene feed.

As indicated by the HDN conversion plots in Figures 2 and 4, the Ni_2P/SiO_2, $Fe_{0.03}Ni_{1.97}P/SiO_2$, $Co_{0.1}Ni_{1.9}P/SiO_2$ catalysts generally exhibit higher carbazole HDN conversions than the sulfided Ni-Mo/Al_2O_3 catalyst over the temperature range 548-673 K, but the difference is greatest at high conversions as noted above. While not a focus of this study, a possible explanation of the lower HDN conversion for the sulfided Ni-Mo/Al_2O_3 catalyst at high temperatures relative to the metal phosphide catalysts is a greater sensitivity to poisoning by NH_3. The catalyst activities are best compared at lower conversions and this is done using the data at 573 K for the carbazole-only feed and at 598 K for the mixed carbazole / benzothiophene feed. The catalyst activities are compared at these temperatures on the basis of mass of catalyst loaded into the reactor (0.25 g), as well as by using turnover frequencies (TOFs) as listed in Table 5. For the TOF calculations, chemisorption capacities (273 K) were used for the metal phosphide catalysts and O_2 chemisorption capacity (196 K) was used for the sulfided Ni-Mo/Al_2O_3 catalyst. On a mass basis, the metal phosphide catalysts have higher carbazole HDN activities than the sulfided Ni-Mo/Al_2O_3 catalyst (except for the $Fe_{0.03}Ni_{1.97}P/SiO_2$ catalyst with the mixed feed), but the sulfide catalyst has a higher TOF at the comparison temperatures. These results point to the inherent limitation of Mo sulfide-based catalysts of having relatively small numbers of active sites, with the low site densities traced to the anisotropic structure of MoS_2 slabs that expose active sites only edge planes. The nickel phosphide based catalysts, on the other hand, have substantially higher active site densities as measured by their chemisorption capacities, which translate into higher carbazole HDN activities despite having lower TOFs.

The HDN activity differences among the three metal phosphide catalysts were generally small, with the Ni_2P/SiO_2 and $Co_{0.1}Ni_{1.9}P/SiO_2$ catalysts somewhat more active than the $Fe_{0.03}Ni_{1.97}P/SiO_2$ catalyst. In earlier work, the bimetallic phosphide compositions were observed to have higher thiophene and dibenzothiophene HDS activities than Ni_2P/SiO_2, which was hypothesized to be due to P-enrichment of the Ni-rich bimetallic phosphide surfaces and transfer of electron density from the Co or Fe to Ni in the phosphides [7,13,24]. As indicated by the surface compositions in Table 2, the $Co_{0.1}Ni_{1.9}P/SiO_2$ and $Fe_{0.03}Ni_{1.97}P/SiO_2$ catalysts are enriched in P at their surfaces (P/M = 1.2-1.5) relative to the Ni_2P/SiO_2 catalyst (P/Ni = 0.68), but no significant differences in catalytic properties are observed. Other than the small HDN activity differences, the $Co_{0.1}Ni_{1.9}P/SiO_2$, $Fe_{0.03}Ni_{1.97}P/SiO_2$ and Ni_2P/SiO_2 catalysts show important similarities – excellent resistance to S incorporation for catalytic measurements using the carbazole / benzothiophene feed and no loss of phase purity as indicated by XRD.

The addition of benzothiophene to the reactor feed inhibited carbazole HDN over the metal phosphide and Ni-Mo/Al_2O_3 catalysts as indicated by the conversion data presented in Figures 2 and 4. Similar inhibition of carbazole HDN by organosulfur compounds was reported for sulfided Mo/Al_2O_3 and Ni-Mo/Al_2O_3 catalysts previously [28,29]. For sulfided Mo/Al_2O_3, carbazole HDN activity decreased with increasing concentrations of S compounds in the feed; the strongest inhibition was observed for dibenzothiophene and carbon disulfide with lesser inhibition for ethanethiol, thiophene and dimethyl sulfide. 2-Methyl-2-propanethiol, when co-fed at levels in the 500-3000 ppm range, reduced the carbazole conversion over a Ni-Mo/Al_2O_3 catalyst by approximately 20 mol% at 603 K, which is similar to the decrease observed in the current study at 598 K (carbazole conversion: 73 mol% - carbazole-only feed, 58 mol% - mixed feed). Nagai et al. concluded that the inhibition of HDN over Ni-Mo/Al_2O_3 was due to the organosulfur compounds competing with carbazole for hydrogenation sites at low temperatures (< 593 K) and hydrogenated carbazoles competing with the sulfur compounds (including H_2S) for C-N hydrogenolysis sites at higher temperatures (≥ 593 K) [29]. For the Ni_2P/SiO_2, $Co_{0.1}Ni_{1.9}P/SiO_2$ and $Fe_{0.03}Ni_{1.97}P/SiO_2$ catalysts, the decreases in carbazole conversion at 598 K associated with co-feeding benzothiophene were larger (e.g. Ni_2P/SiO_2, carbazole conversion: 89 mol% - carbazole-only feed, 62 mol% - mixed feed) than observed for the Ni-Mo/Al_2O_3 catalyst, indicating a greater sensitivity to the organosulfur compound for the metal phosphide catalysts at this temperature. Only the $Fe_{0.03}Ni_{1.97}P/SiO_2$ catalyst exhibited significant HDN inhibition by benzothiophene at 623 K, at which temperature over 95 mol% of the benzothiophene was converted to hydrocarbon products.

Based on studies of carbazole HDN over Ni-Mo/Al_2O_3 catalysts [3,18,29-31] as well as the present work, the reaction network in Scheme 1 is proposed. For the metal phosphide catalysts (and Ni-Mo/Al_2O_3), insignificant amounts of biphenyl were detected in the reactor effluent indicating that direct denitrogenation (DDN) is an inconsequential contributor to carbazole HDN over the catalysts in this study. On the other hand, hydrogenated carbazoles (4H-CARB, 6H-CARB, 12H-CARB) were observed, particularly at low reaction temperatures, and these are intermediates in the hydrogenation (HYD) pathway for carbazole HDN. Four hydrocarbon products of the HYD pathway were detected – CHB, BCH, HCH and MCPCH – but with BCH and MCPCH composing over 70 mol% of the products. HCH and MCPCH are isomerization products formed via ring opening and ring contraction, respectively, of one of the six-member rings of BCH. A similar product selectivity was observed for unsupported W_2C and Pt-promoted W_2C for carbazole HDN using a mixed carbazole / 4,6-DMDBT feed [32]. Reactions of BCH to give HCH and MCPCH in carbazole HDN over the tungsten carbide catalysts were proposed to involve both metal and Brönsted acid sites [32]. The existence of metal and Brönsted acid sites on the surface of Ni_2P and Co_xNi_2P catalysts was invoked in a study of 4,6-DMDBT HDS [33], for which increased activity via the direct desulfurization pathway was associated with isomerization of the organosulfur compound (methyl migration) to give methyl-substituted DBTs that more readily undergo C-S bond cleavage reactions. The high HDS activity via the DDS pathway was most pronounced for unsupported metal phosphides (e.g. $Co_{0.08}Ni_2P$) having P-enriched surfaces; the higher surface P content resulted in a higher concentration of Brönsted acid sites at the catalyst surface in the form of incompletely reduced P species ($H_xPO_4^{x-3}$) [33]. The Ni_2P/SiO_2, $Co_{0.1}Ni_{1.9}P/SiO_2$ and $Fe_{0.03}Ni_{1.97}P/SiO_2$ catalysts in the current study exhibit varying levels of surface P enrichment and the high MCPCH product selectivities are attributed to the presence of both metal and acid sites at the surfaces of these catalysts. Interestingly, the high selectivities for isomerization products (HCH and MCPCH) are more pronounced for the mixed feed than for the carbazole-only feed, suggesting surface modification due to inclusion of benzothiophene in the feed (e.g. formation of a phosphosulfide surface layer [6,7]) that favors further reaction of BCH on the catalyst surface.

As noted in the results section, the trends in product selectivity are similar in most details for the metal phosphide and Ni-Mo catalysts. The most striking differences are the persistence of hydrogenated carbazoles (~6 mol%) in the products at higher temperatures (623-673 K) over the sulfided Ni-Mo/Al_2O_3 catalyst compared to the metal phosphide catalysts (< 3 mol%) and the substantially higher CHB selectivities of the metal phosphide catalysts. At 623-673 K, the CHB selectivity over the sulfided Ni-Mo/Al_2O_3 catalyst was only 5-13 mol% while over the metal phosphide catalysts it was 10-32 mol%, with the CHB selectivities increasing with temperature in each case. Taken together, these selectivity results suggest that C-N hydrogenolysis of 6H-CARB to give CHB is a more active reaction channel for the metal phosphide catalysts than for sulfided Ni-Mo/Al_2O_3, resulting in higher CHB selectivities and higher HDN conversions. The higher CHB selectivity of the metal phosphide catalysts relative to the Ni-Mo/Al_2O_3 catalyst also results in lower hydrogen consumption, an important consideration for catalyst selection for hydrotreating applications.

5. CONCLUSIONS

The carbazole HDN properties of Ni_2P/SiO_2, $Co_{0.1}Ni_{1.9}P/SiO_2$ and $Fe_{0.03}Ni_{1.97}P/SiO_2$ catalysts were investigated for carbazole-only and mixed carbazole – benzothiophene feeds.

The metal phosphide catalysts exhibited high carbazole HDN activities and out-performed a commercial sulfided Ni-Mo/Al_2O_3 catalyst on a mass of catalyst basis, with the largest differences observed at temperatures at which the HDN conversions were high. Co-feeding of benzothiophene inhibited carbazole HDN over the metal phosphides, but the Ni_2P/SiO_2 and Ni-rich bimetallic phosphide catalysts maintained higher activities than the sulfided Ni-Mo/Al_2O_3 catalyst. The product selectivities of the metal phosphide and sulfide catalysts were similar, except that the sulfided Ni-Mo/Al_2O_3 catalyst yielded more hydrogenated carbazoles while the metal phosphide catalysts produced more of the partially hydrogenated hydrocarbon cyclohexylbenzene. The metal phosphide catalysts favored the isomerization products HCH and MCPCH, formed by ring opening and ring contraction of one of the six-member rings of BCH, respectively, that indicate the presence of metal and Brönsted acid sites on the catalyst surfaces. The Ni_2P/SiO_2 and bimetallic phosphide catalysts exhibited excellent stabilities in the HDN conditions employed (carbazole-only and mixed feeds), as indicated by phase purity, average crystallite size and resistance to sulfur incorporation of the supported metal phosphide particles.

6. ACKNOWLEDGEMENTS

This research was supported by a grant from Shell Global Solutions (U.S.) Inc. The authors acknowledge Dr. Jerimiah M. Purcell of Shell Oil Company for carrying out the GC-MS analyses on samples of the reactor effluent.

7. REFERENCES

1. H. Topsøe, B. Clausen, F.E. Massoth, Hydrotreating Catalysis, in: J.R. Anderson, M. Boudart (Eds.) Catalysis: Science and Technology, Springer-Verlag, Berlin, 1996, pp. 1-310.

2. R. Prins, Hydrotreating, in: G. Ertl (Ed.) Handbook of Heterogeneous Catalysis, 2008, pp. 2695-2718.

3. E. Furimsky, F.E. Massoth, Hydrodenitrogenation of Petroleum, Catal. Rev. Sci. Eng., 47 (2005) 297-489.

4. T.C. Ho, L. Qiao, Competitive adsorption of nitrogen species in HDS: Kinetic characterization of hydrogenation and hydrogenolysis sites, J. Catal., 269 (2010) 291-301.

5. P. Wiwel, B. Hinnemann, A. Hidalgo-Vivas, P. Zeuthen, B.O. Petersen, J.Ø. Duus, Characterization and Identification of the most Refractory Nitrogen Compounds in Hydroprocessed Vacuum Gas Oil, Ind. Eng. Chem. Res., 49 (2010) 3184-3193.

6. S.T. Oyama, T. Gott, H. Zhao, Y.-K. Lee, Transition Metal Phosphide Hydroprocessing Catalysts, Catal. Today, 143 (2009) 94-107.

7. R. Prins, M.E. Bussell, Metal Phosphides: Preparation, Characterization and Catalytic Reactivity, Catal. Lett., 142 (2012) 1413-1436.

8. X. Wang, P. Clark, S.T. Oyama, Synthesis, Characterization and Hydrotreating Activity of Several Iron Group Transition Metal Phosphides, J. Catal., 208 (2002) 321-331.

9. S.T. Oyama, Novel Catalysts for Advanced Hydroprocessing: Transition Metal Phosphides, J. Catal., 216 (2003) 343-352.

10. T. Korányi, Phosphorus Promotion of Ni (Co)-Containing Mo-free Catalysts in Thiophene Hydrodesulfurization, Appl. Catal. A, 239 (2003) 253-267.

11. F. Sun, W. Wu, Z. Wu, J. Guo, Z. Wei, Y. Yang, Z. Jiang, F. Tian, C. Li, Dibenzothiophene Hydrodesulfurization Activity and Surface Sites of Silica-Supported MoP, Ni_2P and Ni-Mo-P Catalysts, J. Catal., 228 (2004) 298-310.

12. S.J. Sawhill, K.A. Layman, D.R. Van Wyk, M.H. Engelhard, C. Wang, M.E. Bussell, Thiophene Hydrodesulfurization over Nickel Phosphide Catalysts: Effect of the Precursor Composition and Support, J. Catal., 231 (2005) 300-313.

13. A.F. Gaudette, A.W. Burns, J.R. Hayes, M.C. Smith, T. Seda, M.E. Bussell, Mössbauer Spectroscopy Investigation and Hydrodesulfurization Properties of Iron-Nickel Phosphide Catalysts, J. Catal., 272 (2010) 18-27.

14. W. Kanda, I. Siu, J. Adjaye, A.E. Nelson, M. Gray, Inhibition and Deactivation of Hydrodenitrogenation(HDN) Catalysts by Narrow-Boiling Fractions of Athabasca Coker Gas Oil, Energy Fuels, 18 (2004) 539-546.

15. W.R.A.M. Robinson, J.N.M. van Gestel, T.I. Korányi, S. Eijsbouts, A.M. van der Kraan, J.A.R. van Veen, V.H.J. de Beer, Phosphorous Promotion of Ni(Co)-Containing Mo-Free Catalysts in Quinoline Hydrodenitrogenation, J. Catal., 161 (1996) 539-550.

16. V. Zuzaniuk, C. Stinner, R. Prins, T. Weber, Transition Metal Phosphides: Novel Hydrodenitrogenation Catalysts, Stud. Surf. Sci. Catal., 143 (2002) 247-255.

17. V. Zuzaniuk, R. Prins, Synthesis and Characterization of Silica-Supported Transition-Metal Phosphides as HDN Catalysts, J. Catal., 219 (2003) 85-96.

18. I.I. Abu, K.J. Smith, HDN and HDS of model compounds and light gas oil derived from Athabasca bitumen using supported metal phosphide catalysts, Appl. Catal. A, 328 (2007) 58-67.

19. I.I. Abu, K.J. Smith, Hydrodenitrogenation of Carbazole over a Series of Bulk Ni_xMoP Catalysts, Catal. Today, 125 (2007) 248-255.

20. S.J. Sawhill, D.C. Phillips, M.E. Bussell, Thiophene Hydrodesulfurization over Supported Nickel Phosphide Catalysts, J. Catal., 215 (2003) 208-219.

21. JCPDS Powder Diffraction File, International Centre for Diffraction Data, Swarthmore, PA, 2000.

22. J.B. Goodenough, Interpretation of Structure and Magnetism in Transition-Metal Pnictides M_2X and $(M_{1-x}M'_x)_2X$, J. Solid State Chem., 7 (1973) 428-447.

23. R. Fruchart, A. Roger, J.P. Senateur, Crystallographic and Magnetic Properties of Solid Solutions of the Phosphides M_2P, M = Cr, Mn, Fe, Co and Ni, J. Appl. Phys., 40 (1969) 1250-1257.

24. A.W. Burns, A.F. Gaudette, M.E. Bussell, Hydrodesulfurization Properties of Cobalt-Nickel Phosphide Catalysts: Ni-rich Materials are Highly Active, J. Catal., 260 (2008) 262-269.

25. S. Kasztelan, T. des Courières, M. Breysse, Hydrodenitrogenation of petroleum distillates : industrial aspects, Catal. Today, 10 (1991) 433-445.

26. R. Iwamoto, J. Grimblot, Influence of Phosphorus on the Properties of Alumina-Based Hydrotreating Catalysts, Adv. Catal., 44 (1999) 417-503.

27. R. Prins, Catalytic Hydrodenitrogenation, Adv. Catal., 46 (2001) 399-464.

28. M. Nagai, T. Masunaga, N. Hana-oka, Hydrodenitrogenation of Carbazole on a Mo/Al_2O_3 Catalyst. Effcts of Sulfiding and Sulfur Compounds, Energy Fuels, 2 (1988) 645-651.

29. M. Nagai, Inhibiting Effect of Sulfur and Oxygen Containing Compounds on Carbazole Hydrodenitrogenation on a $NiMo/Al_2O_3$ Catalyst, Sekiyu Gakkaishi, 36 (1993) 502-506.

30. C. Moreau, C. Aubert, R. Durand, N. Zmimita, P. Geneste, Structure-Activity Relationships in Hydroprocessing of Aromatic And Heteroaromatic Model Compounds over Sulphided $NiO-MoO_3/Al_2O_3$ and $NiO-WO_3/Al_2O_3$ Catalysts: Chemical Evidence for the Existence of Two Types of Catalytic Sites, Catal. Today, 4 (1988) 117-131.

31. F. Sánchez-Minero, J. Ramirez, Kinetic Study of the Reaction System 4,6-DMDBT + Naphthalene + Carbazole, Using $NiMo/Al_2O_3-SiO_2(x)$ Catalysts, Ind. Eng. Chem. Res., 50 (2011) 2671-2677.

32. M. Lewandowski, P. Da Costa, D. Benichou, C. Sayag, Catalytic Performance of Platinum Doped Tungsten Carbide in Simultaneous Hydrodenitrogenation and Hydrodesulphurization, Appl. Catal. B., 93 (2010) 241-249.

33. I.I. Abu, K.J. Smith, The Effect of Cobalt Addition to Bulk MoP and Ni_2P Catalysts for the Hydrodesulfurization of 4,6-dimethyldibenzothiophene, J. Catal., 241 (2006) 356-366.

TABLES

Table 1: Catalyst Characterization Data for as-prepared Catalysts

Nominal Composition	Precursor P/Metal Ratio	Average Crystallite Size(nm)	XPS Surface Composition	BET Surface Area(m^2/g)	Chemisorption Capacity	
					CO (μmol/g)	O_2 (μmol/g)
Ni_2P/SiO_2	0.9	12	$Ni_{1.46}P_{1.00}$	132	113	271
$Fe_{0.03}Ni_{1.97}P/SiO_2$	1.0	15	$Fe_{\leq 0.05}Ni_{0.80}P_{1.00}$	124	103	258
$Co_{0.1}Ni_{1.9}P/SiO_2$	0.9	13	$Co_{\leq 0.05}Ni_{0.66}P_{1.00}$	122	107	248
Sulf. Ni-Mo/Al_2O_3	----	----	----	110	----	65

Table 2: Hydrotreating Activity and Characterization Data for Tested Catalysts – Carbazole-only Feed

Catalyst	Post-HDN Average Crystallite Size(nm)	Carbon Content (wt% C)	Sulfur Content (wt% S)	Carbazole HDN Conversion (%) at 623 K
Ni_2P/SiO_2	12	1.06	----	96
$Fe_{0.03}Ni_{1.97}P/SiO_2$	15	1.10	----	95
$Co_{0.1}Ni_{1.9}P/SiO_2$	13	1.39	----	98
Sulf. Ni-Mo/Al_2O_3	----	1.67	7.10	75

Table 3: Hydrotreating Activity and Characterization Data for Tested Catalysts – Mixed Carbazole / Benzothiophene Feed

Catalyst	Post-HDN Average Crystallite Size (nm)	Post-HDN Catalyst C and S Contents		Conversion (%) at 623 K	
		wt% C	wt% S	Carbazole HDN	Benzothiophene HDS
Ni_2P/SiO_2	15	0.67	0.31	96	98
$Fe_{0.03}Ni_{1.97}P/SiO_2$	16	1.27	0.16	80	96
$Co_{0.1}Ni_{1.9}P/SiO_2$	14	0.88	0.35	94	98
Sulf. $Ni\text{-}Mo/Al_2O_3$	----	1.41	8.56	77	95

Table 4: Carbazole HDN Product Selectivity at 623 K

Catalyst	Sulf. $Ni\text{-}Mo/Al_2O_3$		Ni_2P/SiO_2		$Fe_{0.03}Ni_{1.97}P/SiO_2$		$Co_{0.1}Ni_{1.9}P/SiO_2$	
Feed	CARB	CARB + BT	CARB	CARB + BT	CARB	CARB + BT	CARB	CARB + BT
BP	0.2	0.2	0.1	0.2	0.1	0.2	0.1	0.2
CHB	5.0	6.0	12.9	11.4	13.2	14.9	8.9	11.8
BCH	38.3	29.1	33.4	26.4	33.8	22.4	40.3	22.7
MCPCH	47.8	53.7	48.3	52.5	47.3	52.7	46.0	56.9
HCH	8.7	11.0	5.2	9.5	5.6	9.8	4.7	8.4

Table 5: Carbazole HDN Activities and Turnover Frequencies

Catalyst	Carbazole-only Feed (573 K)		Carbazole / Benzothiophene Feed (598 K)	
	HDN Activity (nmol/g·s)	HDN TOF $(s^{-1}) \times 10^4$	HDN Activity (nmol/g·s)	HDN TOF $(s^{-1}) \times 10^4$
Ni_2P/SiO_2	15.9	1.41	17.4	1.54
$Fe_{0.03}Ni_{1.97}P/SiO_2$	13.2	1.28	13.3	1.29
$Co_{0.1}Ni_{1.9}P/SiO_2$	14.9	1.40	18.4	1.72
Sulf. $Ni\text{-}Mo/Al_2O_3$	10.8	1.67	16.3	2.50

SCHEME CAPTION

Scheme 1: Carbazole HDN reaction network (adapted from [3,19]).

FIGURE CAPTIONS

Figure 1: XRD patterns for as-prepared Ni_2P/SiO_2, $Fe_{0.03}Ni_{1.97}P/SiO_2$ and $Co_{0.1}Ni_{1.9}P/SiO_2$ catalysts.

Figure 2: Carbazole HDN conversion vs. temperature for Ni_2P/SiO_2, $Fe_{0.03}Ni_{1.97}P/SiO_2$, $Co_{0.1}Ni_{1.9}P/SiO_2$ and sulfided Ni-Mo/Al_2O_3 catalysts (carbazole only feed).

Figure 3: XRD patterns for Ni_2P/SiO_2 catalysts (a) in as-prepared form, (b) after carbazole HDN testing, and (c) after carbazole HDN testing with benzothiophene co-feed.

Figure 4: Carbazole HDN conversion vs. temperature for Ni_2P/SiO_2, $Fe_{0.03}Ni_{1.97}P/SiO_2$, $Co_{0.1}Ni_{1.9}P/SiO_2$ and sulfided Ni-Mo/Al_2O_3 catalysts (mixed carbazole / benzothiophene feed).

Figure 5: Benzothiophene HDS conversion vs. temperature for Ni_2P/SiO_2, $Fe_{0.03}Ni_{1.97}P/SiO_2$, $Co_{0.1}Ni_{1.9}P/SiO_2$ and sulfided Ni-Mo/Al_2O_3 catalysts (mixed carbazole / benzothiophene feed).

Figure 6: Carbazole HDN product selectivity vs. temperature for a sulfided Ni-Mo/Al_2O_3 catalyst (mixed carbazole / benzothiophene feed).

Figure 7: Carbazole HDN product selectivity vs. temperature for a Ni_2P/SiO_2 catalyst (mixed carbazole / benzothiophene feed).

Figure 8: Carbazole HDN product selectivity vs. temperature for a $Fe_{0.03}Ni_{1.97}P/SiO_2$ catalyst (mixed carbazole / benzothiophene feed).

Figure 9: Carbazole HDN product selectivity vs. temperature for a $Co_{0.1}Ni_{1.9}P/SiO_2$ catalyst (mixed carbazole / benzothiophene feed).

***Graphical Abstract (for review)**

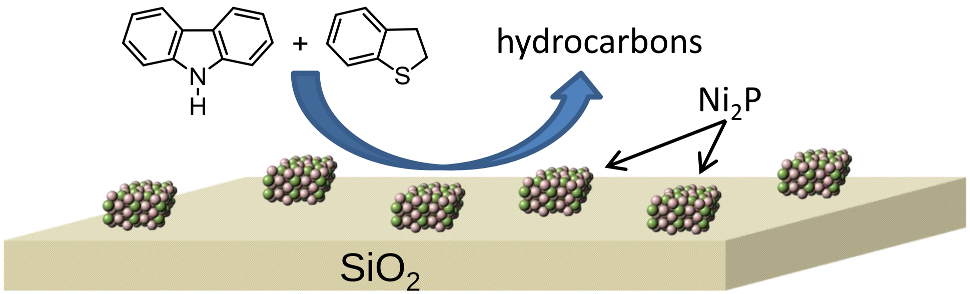

Scheme 1

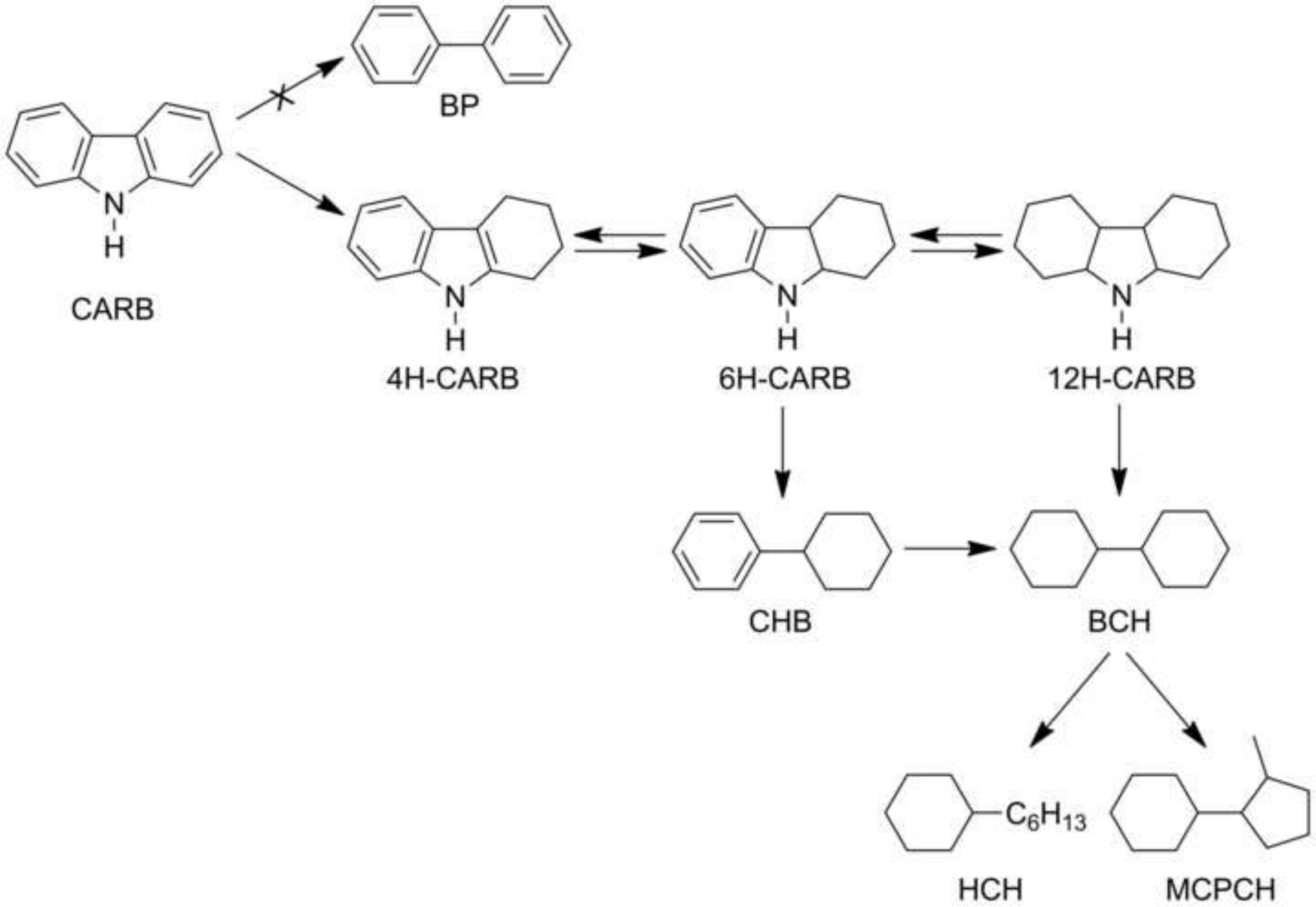

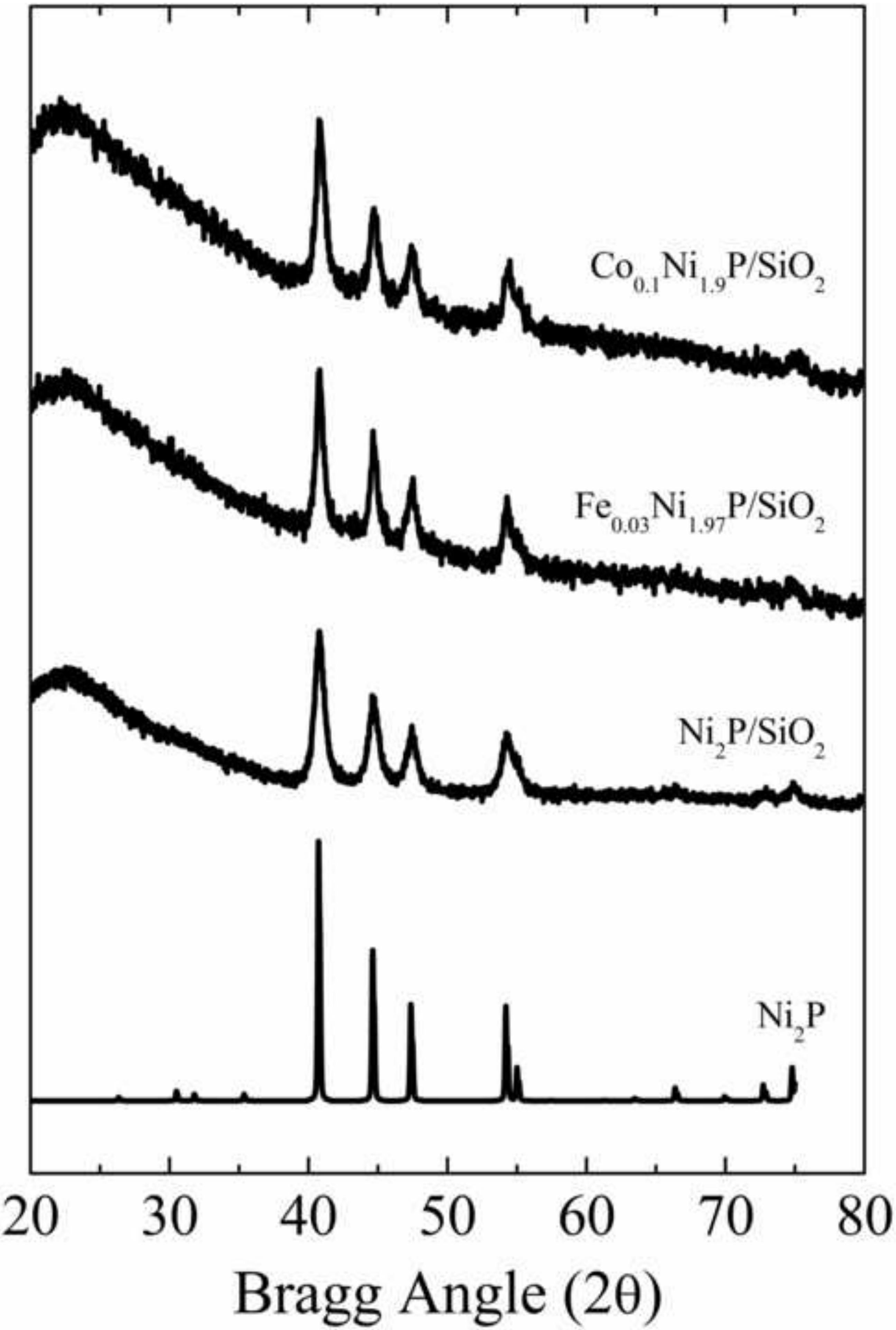
$Co_{0.1}Ni_{1.9}P/SiO_2$
$Fe_{0.03}Ni_{1.97}P/SiO_2$
Ni_2P/SiO_2
Ni_2P
20
30
40
50
60
70
80
Bragg Angle (2θ)

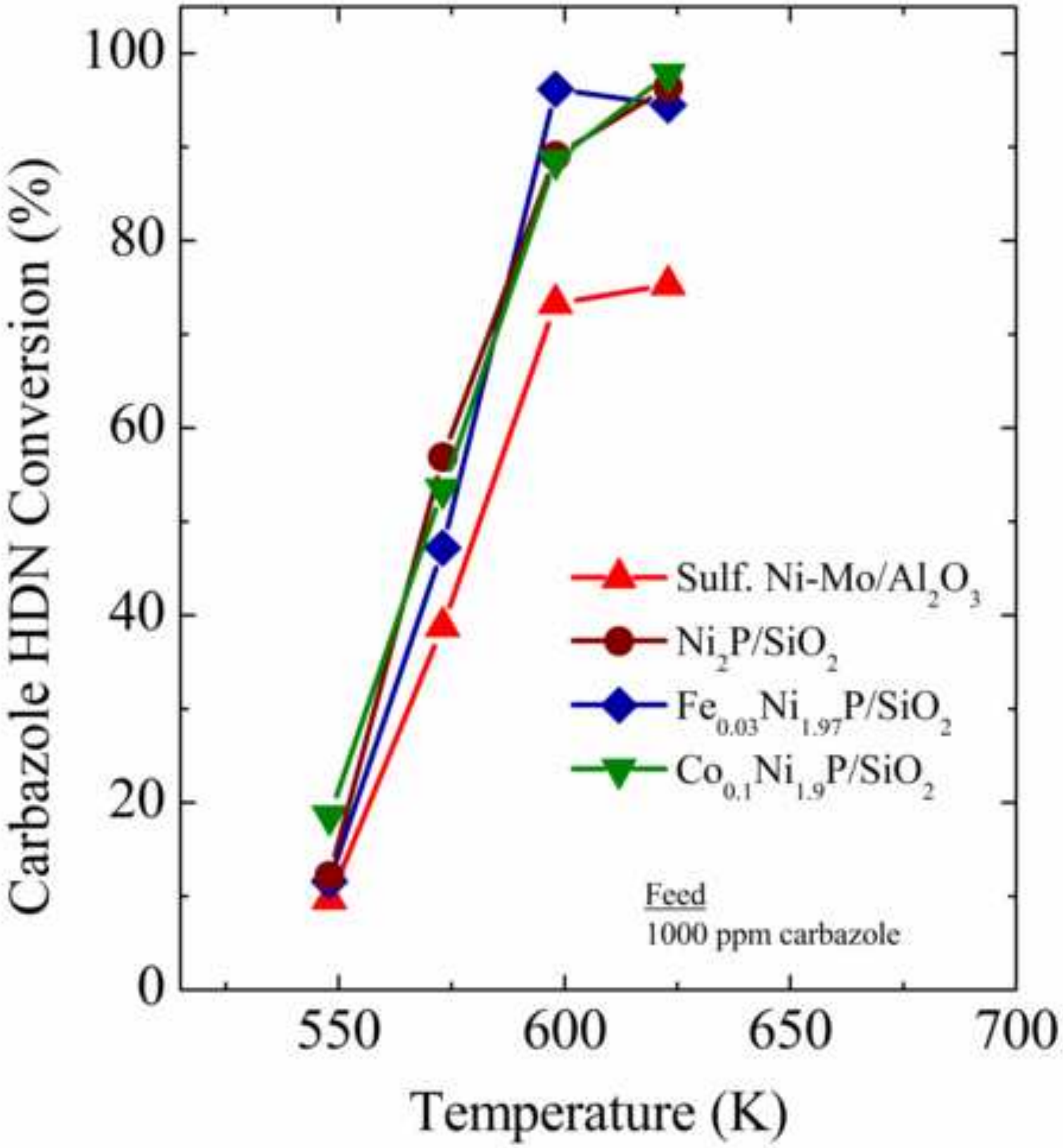
Carbazole HDN Conversion (%)
0
20
40
60
80
100
550
600
650
700
Temperature (K)
Sulf. Ni-Mo/Al_2O_3
Ni_2P/SiO_2
$Fe_{0.03}Ni_{1.97}P/SiO_2$
$Co_{0.1}Ni_{1.9}P/SiO_2$
Feed
1000 ppm carbazole

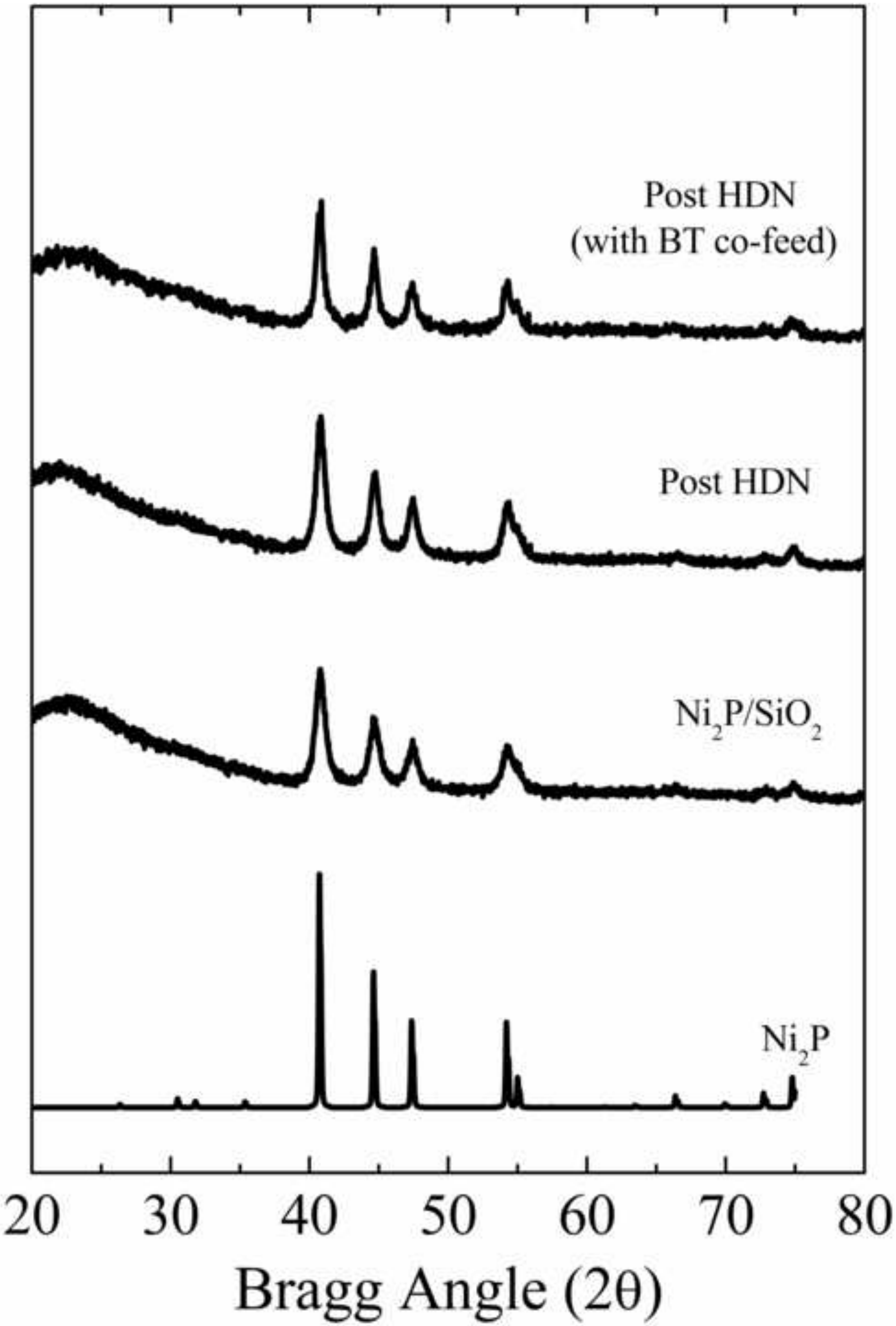
Post HDN
(with BT co-feed)
Post HDN
Ni_2P/SiO_2
Ni_2P
20
30
40
50
60
70
80
Bragg Angle (2θ)

Figure 4

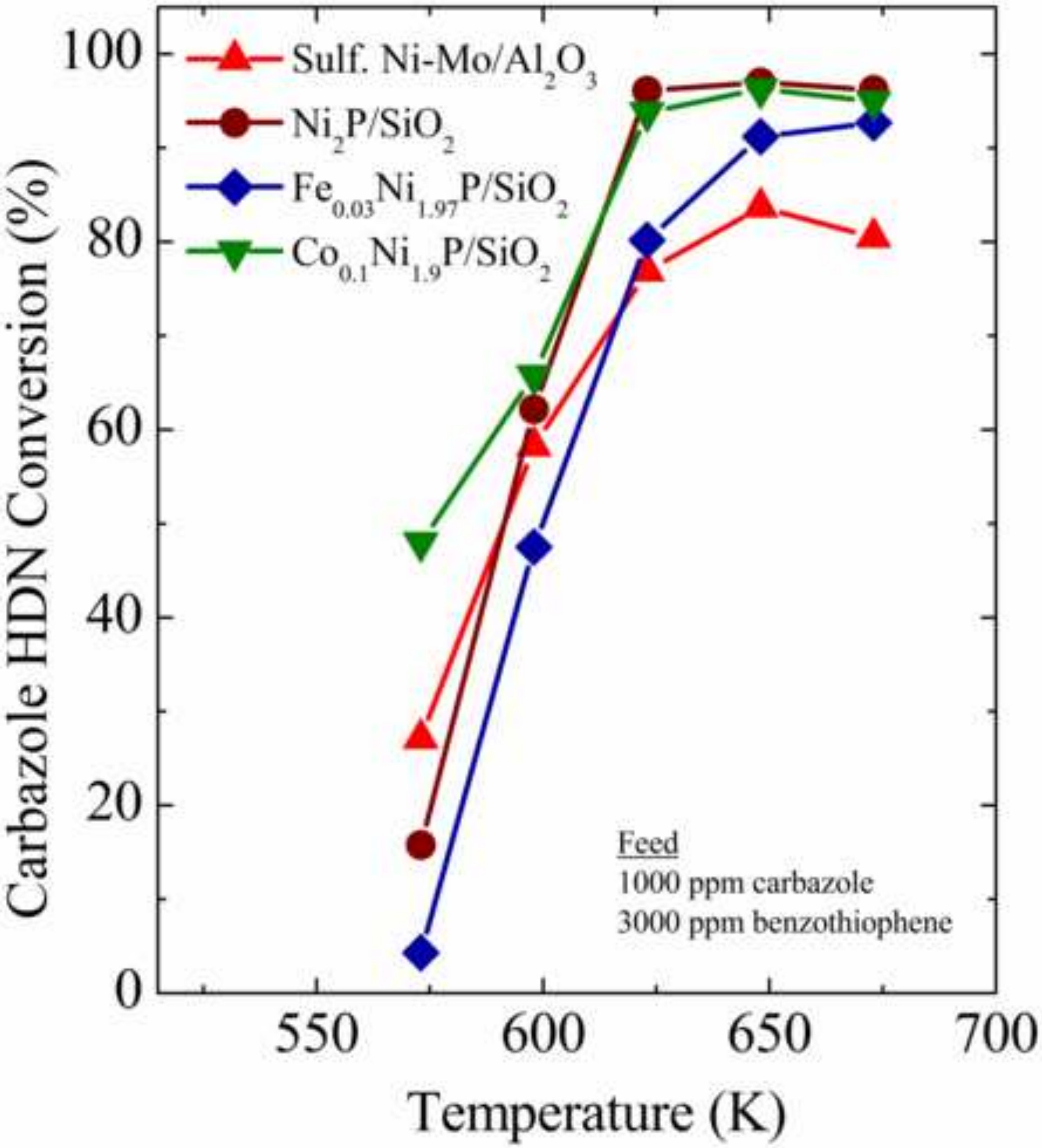
Sulf. Ni-Mo/Al_2O_3
Ni_2P/SiO_2
$Fe_{0.03}Ni_{1.97}P/SiO_2$
$Co_{0.1}Ni_{1.9}P/SiO_2$
Carbazole HDN Conversion (%)
0
20
40
60
80
100
550
600
650
700
Temperature (K)
Feed
1000 ppm carbazole
3000 ppm benzothiophene

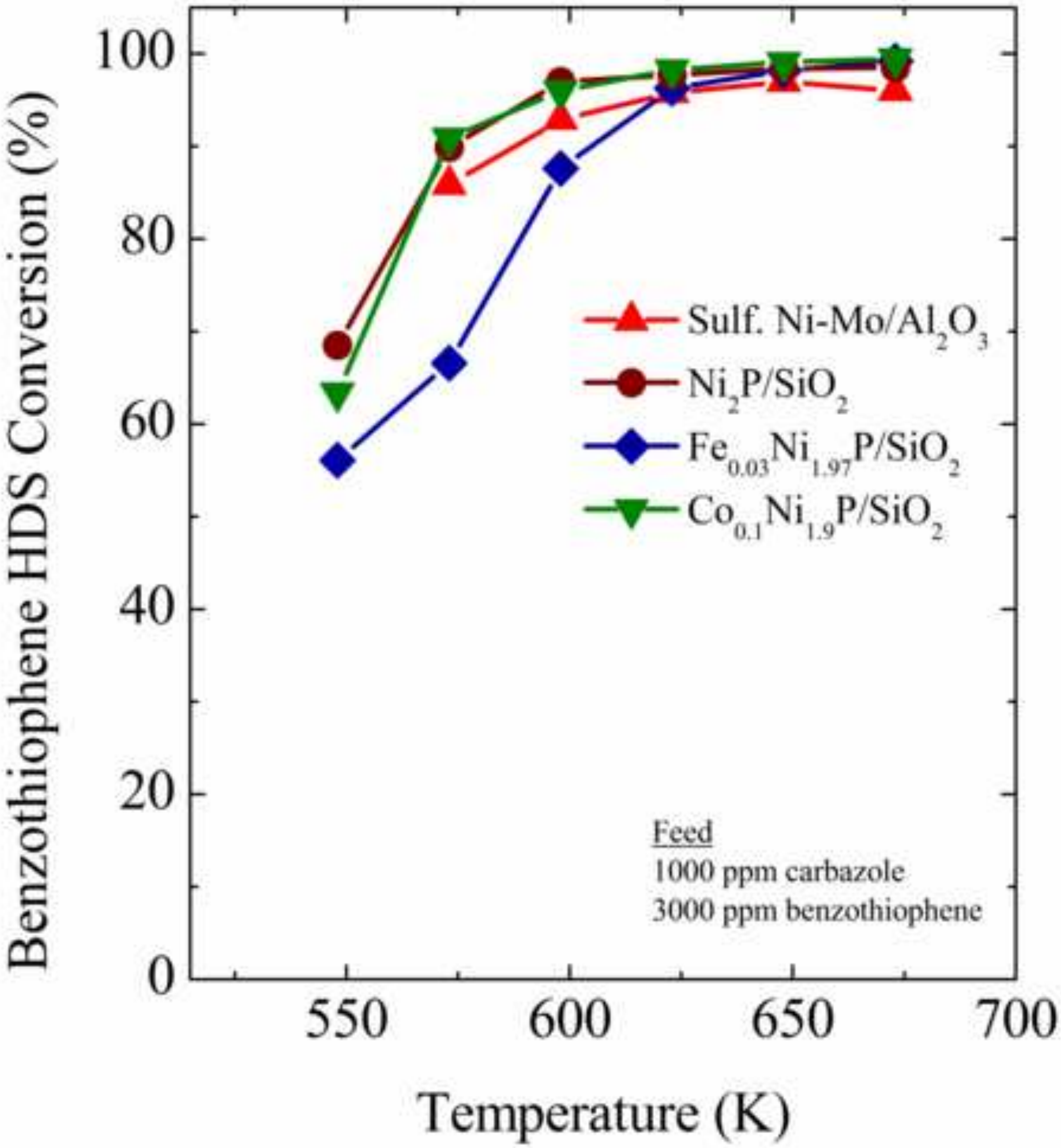
Benzothiophene HDS Conversion (%)
0
20
40
60
80
100
550
600
650
700
Temperature (K)
Sulf. Ni-Mo/Al_2O_3
Ni_2P/SiO_2
$Fe_{0.03}Ni_{1.97}P/SiO_2$
$Co_{0.1}Ni_{1.9}P/SiO_2$
Feed
1000 ppm carbazole
3000 ppm benzothiophene

Figure 6

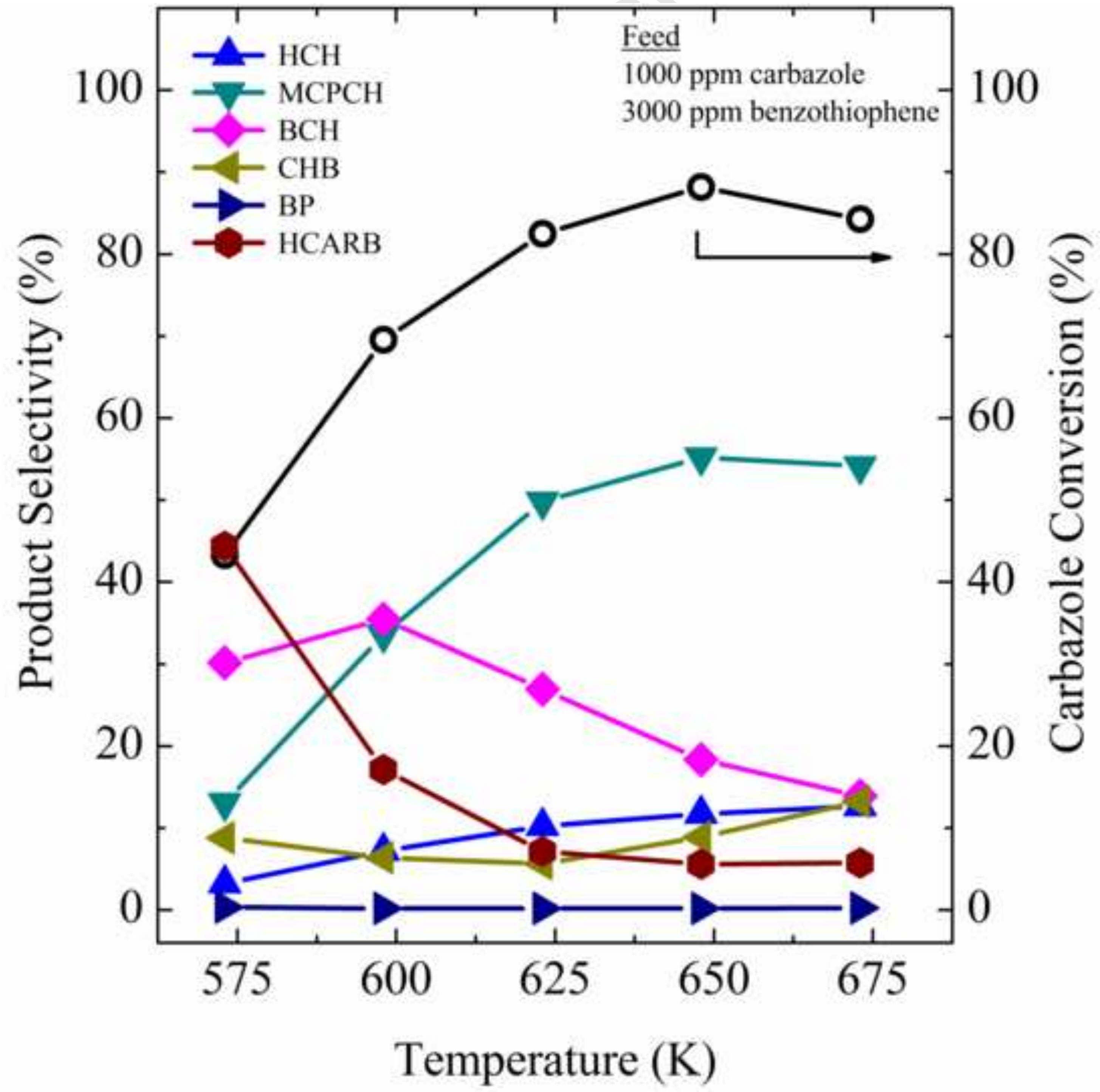

HCH
MCPCH
BCH
CHB
BP
HCARB
Feed
1000 ppm carbazole
3000 ppm benzothiophene
Product Selectivity (%)
Carbazole Conversion (%)
Temperature (K)
0
20
40
60
80
100
575
600
625
650
675

Figure 7

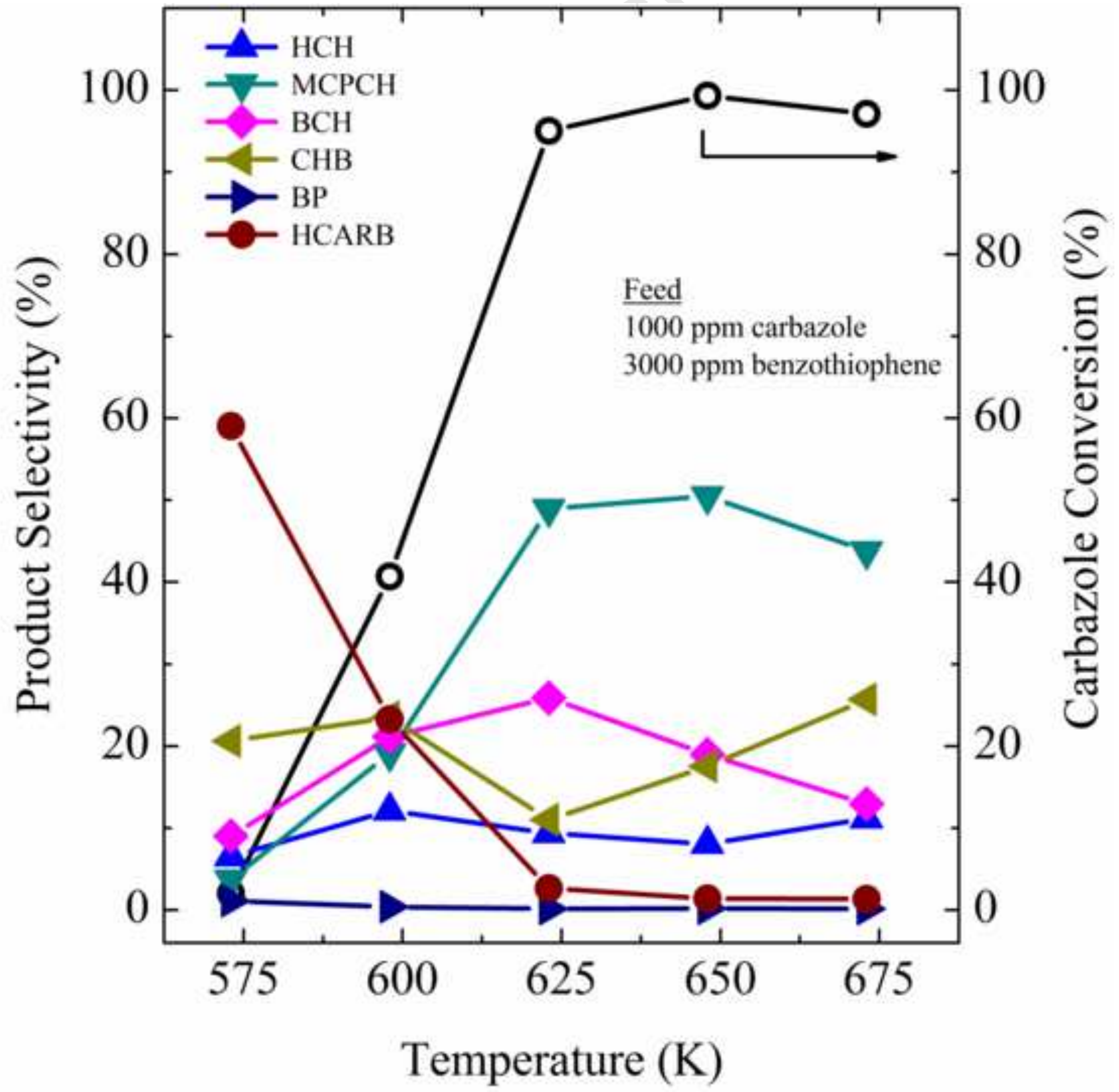
HCH
MCPCH
BCH
CHB
BP
HCARB
Feed
1000 ppm carbazole
3000 ppm benzothiophene
Product Selectivity (%)
Carbazole Conversion (%)
Temperature (K)
0
20
40
60
80
100
575
600
625
650
675

Figure 8

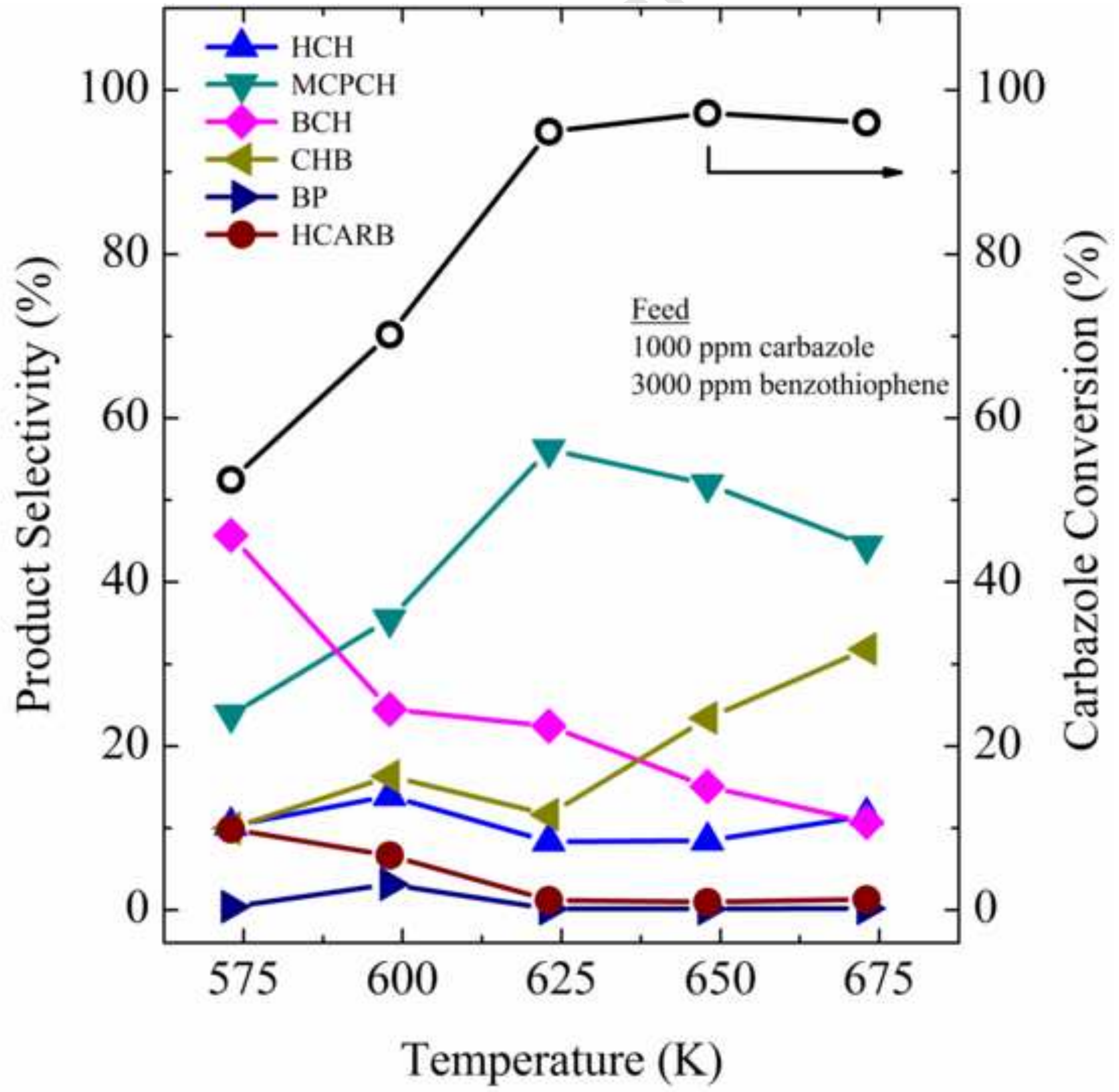
HCH
MCPCH
BCH
CHB
BP
HCARB
Feed
1000 ppm carbazole
3000 ppm benzothiophene
Product Selectivity (%)
Carbazole Conversion (%)
Temperature (K)
0
20
40
60
80
100
575
600
625
650
675

Figure 9

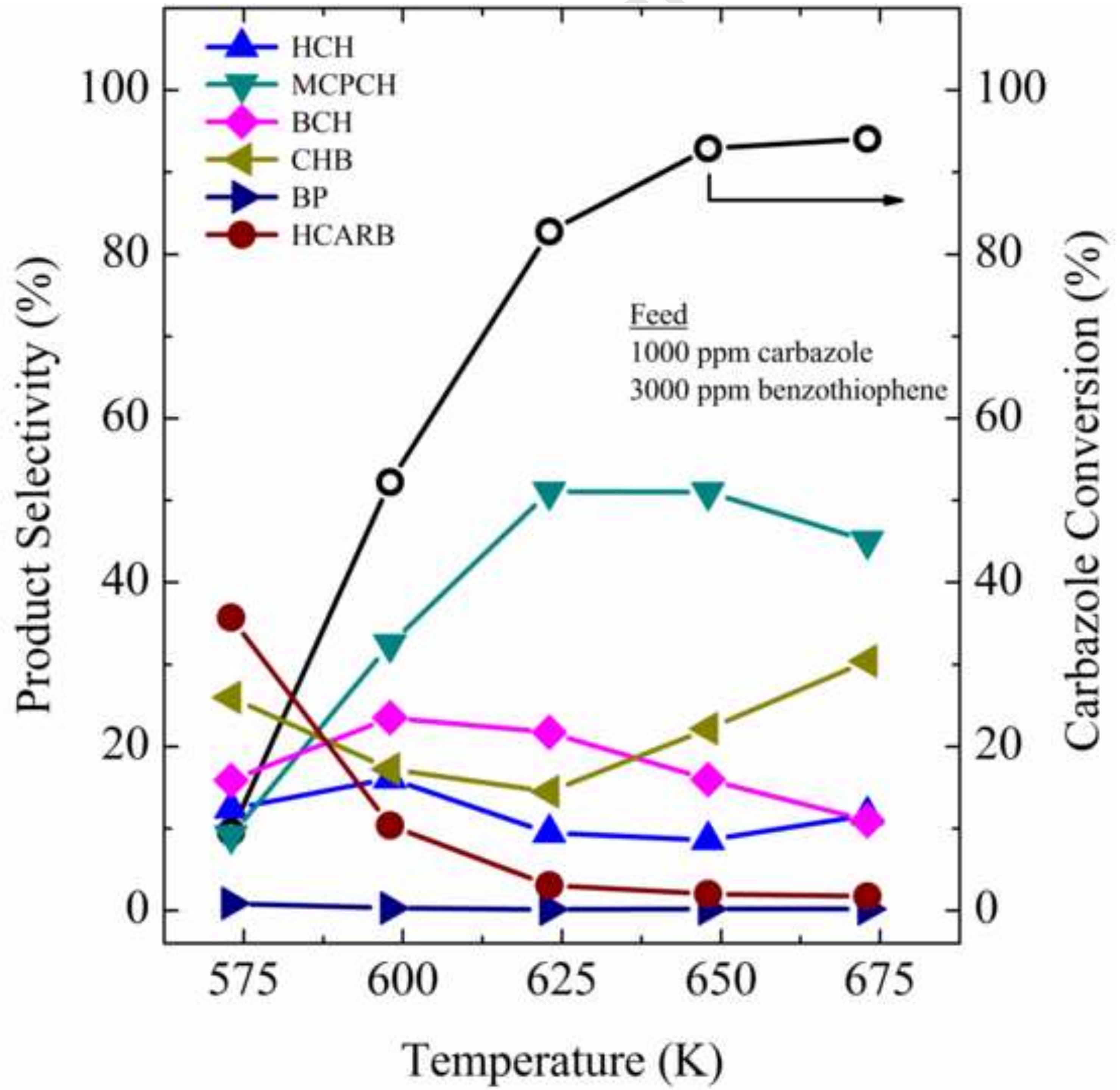

HCH
MCPCH
BCH
CHB
BP
HCARB
Feed
1000 ppm carbazole
3000 ppm benzothiophene
Product Selectivity (%)
Carbazole Conversion (%)
Temperature (K)
0
20
40
60
80
100
575
600
625
650
675